Weak Self-Association in a Carbohydrate System

Trushar R. Patel,* Stephen E. Harding,* Anna Ebringerova,† Marcin Deszczynski,* Zdenka Hromadkova,† Adiaratou Togola,‡ Berit Smestad Paulsen,‡ Gordon A. Morris,* and Arthur J. Rowe*

*National Centre for Macromolecular Hydrodynamics, School of Biosciences, University of Nottingham, Sutton Bonington Campus, Sutton Bonington, LE12 5RD United Kingdom; †Center of Excellence, Institute of Chemistry, Slovak Academy of Sciences, 845 48 Bratislava, Slovakia; and ‡Institute of Pharmacy, University of Oslo, Blindern, Oslo, Norway

ABSTRACT The physiological importance of weak interactions between biological macromolecules (molar dissociation constants >10 μM) is now well recognized, particularly with regard to cell adhesion and immunological phenomena, and many weak interactions have been measured for proteins. The concomitant importance of carbohydrate-carbohydrate interactions has also been identified, although no weak interaction between pure carbohydrate systems has ever been measured. We now demonstrate for the first time to our knowledge using a powerful probe for weak interactions—sedimentation velocity in the analytical ultracentrifuge—that at least some carbohydrates (from the class of polysaccharides known as heteroxylans and demonstrated here to be biologically active) can show well-defined weak self-interactions of the "monomer-dimer" type frequently found in protein systems. The weak interaction between the heteroxylans is shown from a temperature dependence study to be likely to be hydrophobic in nature.

INTRODUCTION

Weak interactions between macromolecules underpin many cellular processes and are particularly important where transient assembly processes and reversible cell adhesion and immunological recognition phenomena are involved (1–4). For example, transient interactions between leucocytes have long been known to be critical for the normal function of the immune system (5,6). Cell-cell adhesion involves the formation of multiple cell adhesion molecule complexes at the cell surface, and if cell deadhesion is to occur, these complexes need to be disrupted. The affinities of cell adhesion molecular interactions must be weak to allow this reversible deadhesion of cell-cell interactions (2,3) and this is precisely what has been observed (7–20). Much of the attention of researchers has been devoted to protein-protein interactions (PPIs) although the significance of carbohydrate-protein interactions (CPIs) and carbohydrate-carbohydrate interactions (CCIs) has also been identified (21).

Molecular interaction strengths are conveniently represented in terms of equilibrium dissociation constants, K_d, whose units are conventionally M, μM, or nM: the larger the K_d the weaker the interaction. Interaction strengths (1) are conventionally regarded as "strong" (K_d < 100 nM), "moderate" (100 nM to 10 μM), or "weak" (>10 μM). The CCIs measured so far have been found to be generally in the "tighter" end of the binding range as compared to PPI/CPIs, and nothing has been observed in the important "weak" region (10*s* and 100*s* of μM level) associated with—and reported for—cell adhesion and immunological phenomena (Table 1). One of the reasons given for the absence of data in this important physiological region has been the difficulty in measuring such interaction strengths in this range (4) although the greater availability of hydrodynamic methods—preferred tools for looking at weak interactions (22,23)—now renders this region accessible for study. Using this technology we can now demonstrate for the first time to our knowledge that carbohydrates from a class of polysaccharide known as the heteroxylans can show well-defined weak self-interaction at the level frequently found in protein systems. This observation is particularly interesting in that many of these hemicellulose polysaccharides exhibit immunostimulatory and complement activation properties (24–30). The demonstration that weak interactions are possible in carbohydrates may help toward a proper understanding of the mechanisms involved in such behavior.

Heteroxylans

Hemicelluloses are the second most abundant group of biopolymers on this planet, and of these the heteroxylans are one of the most important polysaccharides of this group. They consist of $\beta(1\rightarrow4)$ linked D-xylopyranosyl residue backbone with side chains of $\alpha(1\rightarrow3)$ linked L-arabinofuranose residues (31) (Fig. 1) and are often conjugated with phenolic acids such as ferulic acid and *p*-coumaric acid (32–35). In the extraction and purification of these polysaccharides, alkali treatment followed by ultrasound-assisted water extraction is normally required to remove starch and proteins (36,37), a process which also reduces the phenolic acid content. Although heteroxylan is mainly used as a dietary fiber, it has recently been reported that heteroxylans can act as immunostimulators and activate human macrophages and that they can inhibit microbial adhesion (25,28–30,38–40).

Submitted November 11, 2006, and accepted for publication March 14, 2007.

Address reprint requests to Prof. Stephen E. Harding, NCMH, School of Biosciences, University of Nottingham, Sutton Bonington, LE12 5 RD UK. Tel.: 44-11-5951-6148; Fax: 44-11-5951-6142; E-mail: steve.harding@nottingham.ac.uk.

Editor: Jill Trewhella.

0006-3495/07/08/741/09 $2.00

doi: 10.1529/biophysj.106.100891

TABLE 1 Summary of the range of molecular interactions in biological systems

Interaction	Strength, K_d
Enzyme inhibitor:enzyme	~0.01 nM
Cytokine:receptor	~1 nM
Antibody:antigen	~10 nM
Cell-cell recognition molecules	10–200 μM
CD2:CD58	~10 μM (14)
2B4:CD48	10 μM (16)
KIR:MHC I	10 μM (18,19)
CD28:CD86	20 μM (17)
CD2:CD48	50 μM (15)
CD8:MHC class I	50–200 μM (7–11)
CD4:MHC class II	>200 μM (12,13)

For other interactions, see van der Merwe and Davis (3).

Three heteroxylans (PO2, PO5, PO6) were chosen with different bioactivities (Fig. 2) and different severities of extraction (PO6>PO5>PO2). The particular approach we have adopted to investigate possible self-association phenomena in these substances is sedimentation velocity analytical ultracentrifugation (41).

Polysaccharides are more difficult molecules to study compared to proteins because of their polydispersity (i.e., they are characterized by sedimentation coefficient distributions rather than by single values). But provided that the average sedimentation coefficient, s_w, can be reasonably defined, this enables us to study the effect of variation in solute concentration on s_w and thus help us assess associative behavior in terms of K_a—the molar association constant, or more conventionally, K_d. Such a computation requires that nonspecific or ''nonideality'' interaction effects (42) need to be taken into account. We take advantage of newly written software to achieve optimal fitting via a nonlinear least squares (Levenberg-Marquadt (43)) approach, improving on a ''trial and error'' fitting algorithm approach used earlier to study the weak interaction between the cell adhesion molecules CD2 and CD48 (15).

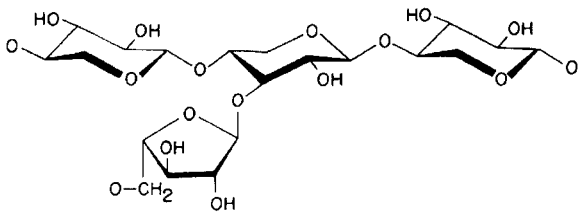

FIGURE 1 Chemical structure of heteroxylan (from Fincher and Stone (31)). The linear backbone of the (cereal) heteroxylan chains consists of β-(1→4)-linked D-xylopyranosyl residues (Xyl*p*) to which single α-L-arabinofuranosyl residues are attached at position 3 and/or both 2 and 3 positions of the Xyl*p* residues as well as a small amount of 2-linked α-D-glucuronopyranosyl uronic acid units. Some galactose- and glucose-containing disaccharide side chains are found as well as phenolic acids (ferulic acid, *p*-coumaric acid, etc.), which esterify the arabinofuranosyl residues at position C-5.

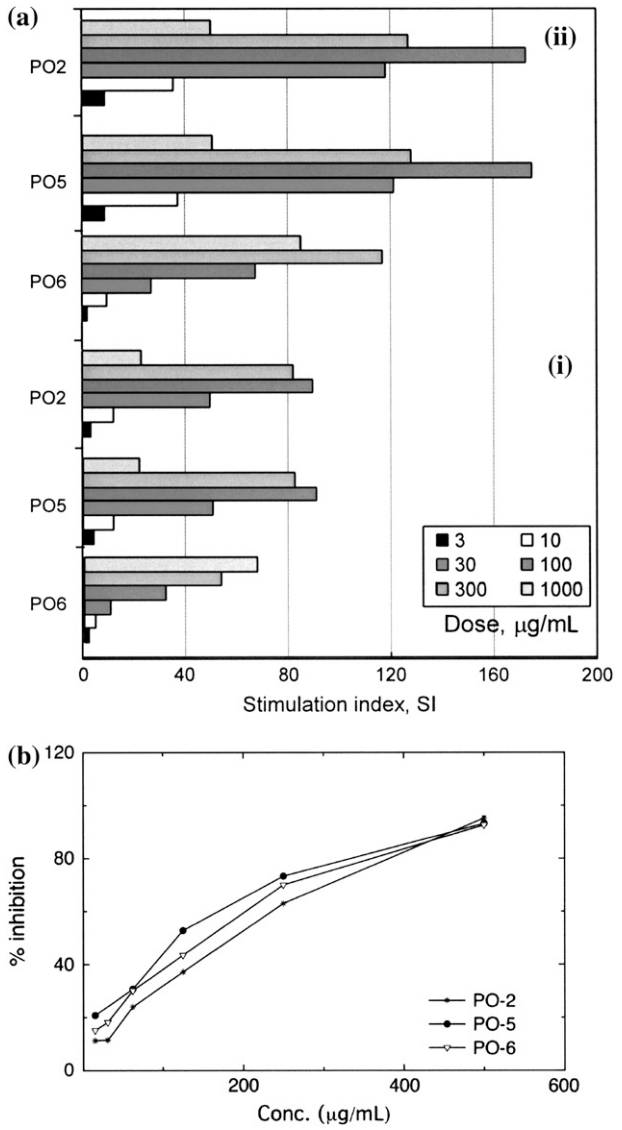

FIGURE 2 Bioactivity of heteroxylans PO2, PO5, and PO6. (*a*) Lymphocyte activation test for heteroxylans (*i*) mitogenic activity, and (*ii*) comitogenic activity. The test is essentially as described by Iribe and Koga (49) adapted for plant polysaccharides (29,50). (*b*) Complement fixation activity of heteroxylans. Based on the procedure of Michaelsen et al. (51) and Nergard et al. (52).

MATERIALS AND METHODS

Heteroxylans

Samples PO2, PO5, and PO6 were prepared from wheat bran by the multistep extraction procedure described by Hromádková and co-workers (44). After separation of mechanically nonremoved starch particles from wheat bran by cold water decantation, the destarched bran (PO) was treated in succession with 1% NH_4OH and 0.5% NaOH at room temperature for 2 h, yielding the fraction known as PO2 and after dialysis used to separate salts and low-molecular products. The destarched bran was refluxed with isopropanol and the residue was successively treated with pectinase in acetate buffer of pH 6.1 at 25°C for 52 h and then finally heated at 100°C for 15 min to solubilize pectic substances. A part of the solid residue was extracted

using 0.5 M NaOH at room temperature for 2 h, and from the extract fraction PO5 was recovered by dialysis of the neutralized extract and then freeze-dried. From the second part of the residue, fraction PO6 was prepared by the same procedure but with saturated $Ca(OH)_2$ as the extracting agent.

Before all experiments, samples were dissolved in a phosphate-chloride (pH 7.0, $I = 0.1$ M) buffered solution (45) in screw-capped tubes with constant stirring at low speed. During this period, the temperature was raised to 80.0°C for 10 min to obtain maximum solubility. Stirring continued at room temperature (20.0°C) overnight at low speed. Samples were then subjected to preparative centrifugation at 40,000 rpm for 15 min (Beckman L8-55 M Ultracentrifuge, Beckman Instruments, Palo Alto, CA) to remove any insoluble particles or aggregates. Solution concentrations were estimated using a differential refractometer (Atago DD5, Jencons Scientific, Leighton Buzzard, UK) and a refractive index increment, dn/dc, of 0.151 mL/g (46).

Composition analysis

Residual protein content was calculated as percentage nitrogen × 6.25 using an Elemental Analyser (Perkin-Elmer, Model 240, Wellesley, MA). Samples were hydrolyzed in 2 M TFA (2,2,2 trifluoroacetic acid) for 2 h to measure the monosaccharide composition (47) using article chromatography and gas-liquid chromatography of alditol trifluoroacetates (Hewlett-Packard, Model HP 5890, Palo Alto, CA). The amount of feruloyl groups (mg FA/g sample) was determined using a spectrophotometer (48) by direct absorbance measurement at 375 nm of freshly prepared solutions of hemicelluloses (0.5 mg/mL) in 0.07 M glycine-NaOH buffer (pH 10.0) with the Specord M-20 ultraviolet-visible spectrophotometer (Zeiss, Jena, Germany). A calibration curve was constructed using ferulic acid as standard.

Lymphocyte transformation test

The method described by Iribe and Koga (49) was followed to study the level of bioactivity (29,50). Rat thymocytes (strain Wistar, males weighing ~200 g) in Roswell Park Memorial Institute-1640 medium supplemented with 5% fetal calf serum were cultivated at 1.5×10^6 cells in 0.2 mL per well with or without 25 μg/mL of the T-mitogen phytohemagglutinin (PHA). Test compounds were added at final concentrations of 3, 10, 30, 100, 300, and 1000 μg/mL. After 72 h of cultivation, thymocyte proliferation was measured by incorporation of ^{3}H-thymidine expressed in counts per minute (cpm). In each of three independent experiments, mean cpm for each set of four replicas was used to calculate the stimulation indices (SI).

Complement fixation activity

The procedure of Michaelsen et al. (51) and Nergard et al. (52) was followed and is based on the inhibition of hemolysis of antibody-sensitized sheep erythrocytes by human sera. The percentage of inhibition of lysis $= 100 \times (A_{control} - A_{sample}/A_{control})$.

Sedimentation velocity experiments

An Optima XL-I analytical ultracentrifuge (Beckman Instruments) was employed equipped with a Rayleigh interference optical system. Solutions (380 μL)/reference solvent (400 μL) were injected into double sector, carbon-filled 12-mm path length centerpieces and then loaded into an 8-hole titanium rotor. Solutions of PO2, PO5, and PO6 were run at a rotor speed of 40,000 rpm and a temperature of 20.0°C. PO5 solutions were also measured at temperatures of 5.0°C and at 30.0°C. Changes in the concentration distribution in the ultracentrifuge cell as a function of time were analyzed using the so-called least squares $g^*(s)$ methods incorporated into the finite-difference algorithm SEDFIT (53,54), with scans taken every 4 min. Scans were used from attainment of meniscus depletion (typically after 90+ min at 20°C) up to the point at which the midpoint of the boundary had traversed a further ~20% of column length—which meant that ~40 scans were analyzed depending on the temperature of the measurement (more scans were used at 5°C, where the sedimentation rates are slower because of the higher viscosity of the solvent, than at 30°C. A regularization setting was set at 0.68.

The weight average s for a particular component was then corrected to standard solvent conditions (density and viscosity of water at 20°C) to yield $s_{20,w}$ (S) (55). The $s_{20,w}$ was measured at a range of concentration, c, for all samples. The $s_{20,w}$ vs. c dependence was then analyzed using the routine MONOMER-DIMER to yield estimates for the zero concentration or ''ideal'' value $s^0_{20,w}$ and the association constant k_a (mL/g), and hence the molar association constant K_a (μM^{-1}) if the molar mass (molecular weight) M of the monomer species is known. MONOMER-DIMER is a locally written algorithm defined within the software pro Fit (Quantum Soft, Zürich, Switzerland). It derives from the original work of Gilbert and Gilbert (56), adjusted to take into account the hydrodynamic dependence (nonspecific or ''nonideality'' effects) of the (weight-averaged) s value of the sedimenting species (57,58). k_s for the monomer species was computed independently, knowing the molecular weight and $s^0_{20,w}$ values and the partial specific volume. The k_s for the dimer was assumed to be identical, and both were fixed in the fitting (58). The equations employed in this fitting are derived as follows. From the law of mass action, we solve in the conventional manner for the roots of a quadratic expression, thus providing the degree of association (α) of monomer units to dimers, in terms of the total solute concentration, c:

$$A = 2K_a c; \quad B = -(4K_a c + 1); \quad C = 2K_a c, \tag{1}$$

where K_a, the molar association constant, $= 1/K_d$. A, B, and C are related by the following quadratic equation

$$\alpha = (-1)\times(B + (B \times B - 4AC)^{0.5})/2A \tag{2}$$

with

$$c_{monomer} = (1 - \alpha c); \quad c_{dimer} = \alpha c \tag{3}$$

and from which we compute relevant s values over all c values to be fitted:

$$s_{monomer,c} = s^0_{monomer}(1 - k_s c - ((c^2 V_s^2(2\phi_p - 1))/(\phi_p^2)))/(k_s c - 2cV_s + 1) \tag{4}$$

$$s_{dimer,c} = s^0_{dimer}(1 - k_s c - ((c^2 V_s^2(2\phi_p - 1))/(\phi_p^2)))/(k_s c - 2cV_s + 1), \tag{5}$$

where $s^0_{monomer}$ and s^0_{dimer} are the sedimentation coefficients at infinite dilution of the monomer and dimer species, respectively, V_s is the swollen specific volume of the species (taken here as 1.4 mL/g), and ϕ_p is the maximal packing volume, assumed to be identical for both species and taken as equal to 0.45 v/v (the precise value assumed is virtually irrelevant for fitting of these dilute solutions).

The weight-averaged sedimentation coefficient (s_w, in which the subscript ''w'' denotes the nature of the average) at (total) concentration, c, is then given by

$$s_{w,c} = (c_{monomer,c} \times s_{monomer,c} + c_{dimer,c} \times s_{dimer,c})/c, \tag{6}$$

and in the function MONOMER-DIMER we carry out a conventional fit (Eqs. 1–6) within pro Fit with initial values chosen by manual fitting and final results obtained via a Marquadt-Levenberg algorithm, which returns error estimates for the parameter K_a. In these analyses K_a and $s^0_{monomer}$ are floated as variables. The s^0_{dimer} value was computed from $s^0_{monomer}$ on the assumption that to an approximation, $s^0_{dimer} \sim s^0_{monomer} \times 2^{2/3}$. By varying this calculated s^0_{dimer} value over a range, it was shown that the level of

variation in K_a estimates resulting was within the size exclusion of the estimate of K_a (as is expected for weak interaction). The values for k_s for the monomer (typically close to 22 mL/g at 20°C) were computed from the equation of Rowe (42):

$$k_s = 2\bar{v}(V_s/\bar{v} + (f/f_0)^3) \quad (7)$$

using vales of 0.63 mL/g for the partial specific volume and 1.4 for the swelling ratio $V_s/\bar{v}$. The frictional ratio was computed conventionally from the molecular weight, sedimentation coefficient, and partial specific volume via the software package BIOMOLS (http://www.nottingham.ac.uk/ncmh). Finally, an estimate for K_d was obtained from the reciprocal of K_a.

The above theory has been derived for the case of a single monomeric species, undergoing association to the dimer level, the resultant mixture being characterized by its weight-averaged sedimentation coefficient. Clearly in our case, where we have a polymeric species of narrow distribution, we have a whole set of self-interactions taking place. However, since the weight-averaged s value of two distributions, each of which is a weight-averaged distribution must, of algebraic necessity, be itself a weight-averaged value over the whole distribution, we consider that the approach will be valid to a level more than adequate for making an ''interaction/no interaction'' judgment and to giving a reasonable estimate for its strength. We have also assumed the interaction is monomer-dimer and proceeds no further within the concentration range (limited by the solubility of the polysaccharide) studied. If the association were to proceed indefinitely, because of the weakness of the association the levels of n-mers higher than dimer would not be significant.

Molecular weight determination

A value for the (weight average) molecular weight M_w for each of PO2, PO5, and PO6 was required to enable conversion of k_d values to molar dissociation constants, K_d. Size exclusion chromatography (SEC) coupled with multiangle laser light scattering (MALLs) was used. The chromatographic assembly consisted of an high-performance liquid chromatography pump (Model PU-1580, Jasco, Tokyo, Japan), a Rheodyne injection valve (Model 7125, Rheodyne, St Louis, MO) fitted with a 100-μL loop, a Phenomenex guard column (Phenomenex, Macclesfield, UK), TSK (Tosoh Bioscience, Tokyo, Japan) Gel G4000 PW connected in series with TSK Gel G3000 PW. The angular scattering envelope was recorded using a Dawn DSP MALL photometer, and concentration was determined using an Optilab 903 interferometric refractometer (both instruments from Wyatt Technology, Santa Barbara, CA) with phosphate buffer saline as mobile phase. The SEC-MALLs system was equilibrated overnight with the phosphate-chloride buffer at flow rate of 0.8 mL/min and room temperature. Samples (100 μL) with accurately know concentration and filtered through 0.45-μm filters (Whatman, Maidstone, UK) were injected at the same flow rate. The primary data obtained from the light scattering photometer and the refractometer were captured and analyzed on a PC using the ASTRA (for Windows 98) software supplied by the manufacturer. Because of the low injection concentrations (<1.7 mg/mL) used followed by considerable dilution on the columns, thermodynamic nonideality effects were not taken into consideration.

RESULTS AND DISCUSSION

Integrity and bioactivity

The monosaccharide composition of the PO2, PO5, and PO6 fractions is summarized in Table 2. Using the data from Table 2, the ratio of arabinose/xylose was calculated to give values of 0.73, 0.89, and 0.86 for PO2, PO5, and PO6, respectively. In addition to arabinose and xylose, all the fractions contain considerable amount of glucose and very small amount of galactose and rhamnose. The amount of ferulic acid was also measured using spectrophotometer, with the highest levels detected in the PO5 fraction. Only small amounts of protein impurity were detected, as manifested by the low levels of nitrogen.

Both mitogenic-comitogenic and complement fixation experiments (Fig. 2 *a*) showed that all three preparations of heteroxylan were bioactive but to different extents. The direct mitogenic effect was expressed as SI_{mit} = mean cpm for test compound/mean cpm for the control without stimulant. The comitogenic effect was expressed as SI_{comit} = mean cpm (test compound + PHA)/mean cpm for PHA. The mean cpm for control cultures without any addition was 924 (704–1143). For cultures incubated with PHA, the mean cpm was 1341 (1081–1601). The eventual contamination of the samples by endotoxin was checked in a parallel test performed in the presence of polymyxin B, which inhibits the biological effects of endotoxin including its mitogenic activity (59); this was negative for all our samples. These results are reinforced by the complement fixation activity experiments for the heteroxylans. In Fig. 2 *b* dose-dependent response curves are used to represent the concentration of test sample able to give 50% inhibition of lysis (ICH50), where low ICH50 means high complement fixing activity. Here, low ICH50 means high complement fixing activity. It is evident from Fig. 2 *b* that all three samples show clear activity.

Sedimentation velocity and molar dissociation constants

The sedimentation distribution profiles for PO2, PO5, and PO6 revealed a nearly quasicontinuous distribution, confirming the integrity of the sample preparation procedure (Fig. 3). The distributions shown with s (Fig. 3 *a*) and $\log(s)$ (Fig. 3 *b*) as the abscissae are apparent ones as they are not corrected for diffusion or nonideality effects. The latter plot

TABLE 2 Composition analysis of heteroxylans PO2, PO5, and PO6

Sample	PH	FA	Neutral sugar composition (mass %)							Ara/Xyl molar ratio
	(%)	mg_{FA}/g	Rha	Fuc	Ara	Xyl	Man	Glc	Gal	
PO2	9.8	19.9	-	-	38.8	53.1	0.9	3.4	3.8	0.73
PO5	7.4	32.3	1.1	1.9	44.6	50.3	-	2.1	-	0.89
PO6	8.4	27.1	0.8	-	44.1	51.3	0.7	3.1	4.0	0.86

The protein content (% $N \times 6.25$) of the samples was <0.5%. PH, phenolics determined as ethylacetate extract after alkaline hydrolysis (81); FA, ferulic acid, determined according to Izydorczyk and Biliaderis (48).

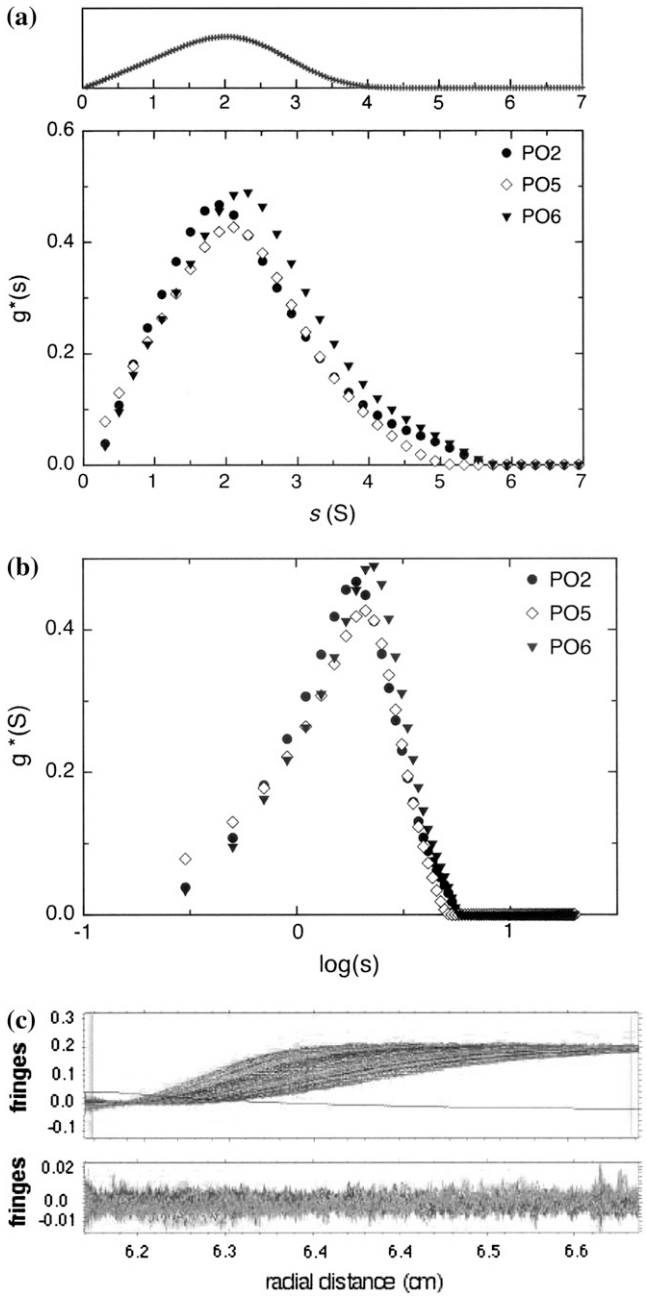

FIGURE 3 Plots of (*a*) $g^*(s)$ vs. s (S) and (*b*) $g^*(s)$ vs. log(s) for PO2 (0.85 mg/mL), PO5 (0.75 mg/mL), and PO6 (0.85 mg/mL) at 20.0°C. All experiments performed at 20.0°C at a rotor speed of 40,000 rpm. (*c*) Fitted radial concentration distributions for PO5 at 20°C superimposed on raw data (*upper*) and distribution of residuals (*lower*). Scans were taken every 4 min, other details as text. The single solid line is the time-independent noise distribution or ''baseline''.

is also shown since polysaccharides usually exhibit a log-normal distribution with regard to molecular weight (although we do not know the functional dependence of s with M for these polysaccharides). The so called c(s) procedure popularly used in protein work for correcting for diffusion is not applicable here since the assumption of a single frictional ratio is invalid. Simulations of the g*(s) vs. s profiles were performed based on what would be the expected distribution for an ideal monodispersed monomer species with no self-association (i.e., the breadth of the distribution being solely due to translational diffusion); such a simulation is shown in Fig. 3 *a*, top. Comparison of the experimental $g^*(s)$ s profile with that generated from a simulated ideal data for a monomeric system shows that the former profile is a little broader than the latter and a little more ''skewed'' toward the upper end. This is exactly what would be expected for a simple monomer-dimer system, on the basis of Gilbert and Gilbert theory. Essentially, the polydispersity of the system is so low that it would actually be difficult, on the basis of our results, to say with any certainty that the system is other than quasi-monodisperse, and this is supported by the lack of symmetry when we plot $g^*(s)$ log s (Fig. 3 *b*); a more symmetrical distribution would be expected for a broader log-normal distribution of molecular species. In regard to the possible presence of higher n-mers of the (narrowly distributed with respect to mass) base species (plural), we note that the $g(s)$ profile returns to the baseline in the region above ~5S, where any such higher species should contribute. This is clear evidence for their absence on any significant scale. Thus we are not identifying an interaction which is other than weak; this implies that at our working concentrations the greater number of the species present in our narrow distribution of monomers will be in the nonassociated state.

The weight average sedimentation coefficient of all three samples at 20.0°C and of PO5 at 5.0°C as well as 30.0°C were then corrected to the sedimentation coefficient under the standard conditions of the density and viscosity of water at 20.0°C, $s_{20,w}$. It was observed from plots for PO2 and PO5 that the sedimentation coefficient ($s_{20,w}$) values tended to increase as the concentration is elevated (Fig. 4, *a* and *b*), with this tendency in the order PO2>PO5. As this is an effect of the opposite sign to what is predicted on the basis of nonspecific interaction (above), we can be confident that a specific interaction must be present, at least for PO2 and PO5. PO6 by contrast appeared to show more normal behavior (Fig. 4 *c*). Since a self-association is evident, the data of Fig. 4 were then fitted using the algorithm MONOMER-DIMER to yield estimates for $s^0_{20,w}$ and k_d, the dissociation constant (g/mL), and the data are presented in Table 3. To convert k_d values to molar dissociation constants, K_d, we use the weight average M_w from SEC-MALLs (~32,700 g/mol) for all samples. PO2 and PO5 are classical ''weak'' interactions (K_ds ~340 and 660 μM, respectively), with PO6 showing little or no interaction ($K_d > 3000$ μM).

Effect of temperature

In Fig. 5 we explored the effect of temperature on the self-association. To facilitate the comparison (performed on PO5), plots were of $s_{20,w}/s^0_{20,w}$ versus concentration. The ''monomer'' and ''dimer'' lines refer to the 30.0°C sample, which

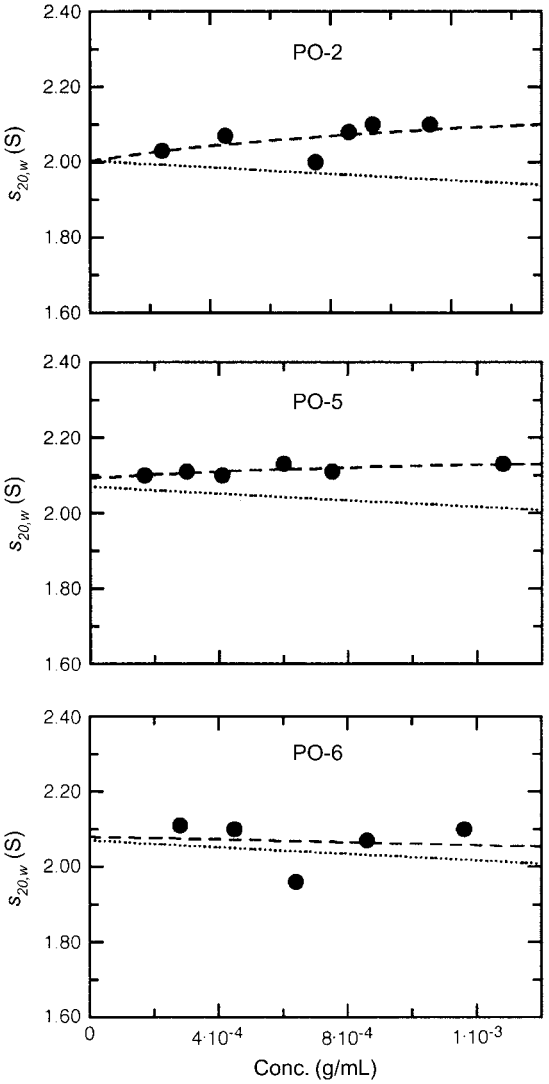

FIGURE 4 Change in apparent sedimentation coefficient, $s_{20,w}$, with concentration (corrected for radial dilution) for PO2, PO5, and PO6. The broken lines are fits given by the function MONOMER-DIMER. The dotted lines are the theoretical concentration dependencies for monomers with no self-association.

shows the highest degree of *s-c* dependence as a consequence of its elevated frictional ratio. The corresponding ''monomer'' and ''dimer'' lines for the 5.0°C and 20.0°C data are omitted in the interest of clarity: they are much less steep than the 30.0°C lines. Interestingly the highest degree of self-association occurred at 30.0°C with a K_d of ~140 μM

TABLE 3 Measured dissociation constants K_d

Samples	Temp (° C)	$s^0_{20,w}$ (S)	k_d (*g*/mL)	K_d (μM)
PO2	20.0	2.10 ± 0.05	0.011	340 ± 50
PO5	5.0	2.60 ± 0.02	>0.100	>3000
PO5	20.0	2.20 ± 0.01	0.020	660 ± 20
PO5	30.0	1.80 ± 0.04	0.004	140 ± 40
PO6	20.0	2.20 ± 0.04	>0.100	>3000

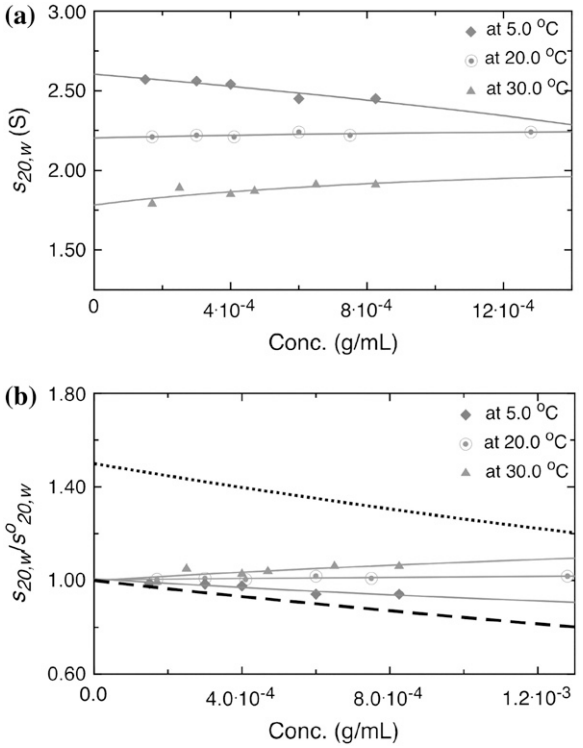

FIGURE 5 Effect of temperature on the change in (*a*) apparent sedimentation coefficient $s_{20,w}$ and (*b*) $s_{20,w}/s^0_{20,w}$ with concentration (*c*) for PO5 at 5.0°C, 20.0°C, and 30.0°C. The ''monomer'' (*dashed*) and ''dimer'' (*dotted*) lines refer to the 30.0°C sample.

whereas, at 5.0°C, there was no significant self-interaction ($K_d > 3000$ μM).

CONCLUSION

It is clear that the heteroxylan samples exhibit weak but definite self-association phenomena in the order PO2>PO5> PO6, an order corresponding to different severities of treatment, with no evidence of statistically significant association for PO6. Temperature dependence studies indicate that the interaction is hydrophobic in nature, with increasing temperature increasing the strength of the interaction (60), and the converse for lowering the temperature with no evidence of statistically significant association for PO5 when the temperature is as low as 5°C; there may be hydrophobic or sticky patches on the polysaccharide backbone causing neighboring molecules to associate in a weak or transient fashion (Fig. 6). Hydrophobic interactions are not unexpected in polysaccharides since they can be amphiphilic in nature, possessing both hydrophobic (carbon/hydrogen atoms) and hydrophilic (oxygen-possessing) faces. It has been suggested that ''CCIs rely on this amphiphilicity as the driving force for association, largely by removing the hydrophobic faces from bulk aqueous solution'' (61,62). What is unexpected is the weakness of the interaction—polysaccharides generally interact either strongly or not at all (63).

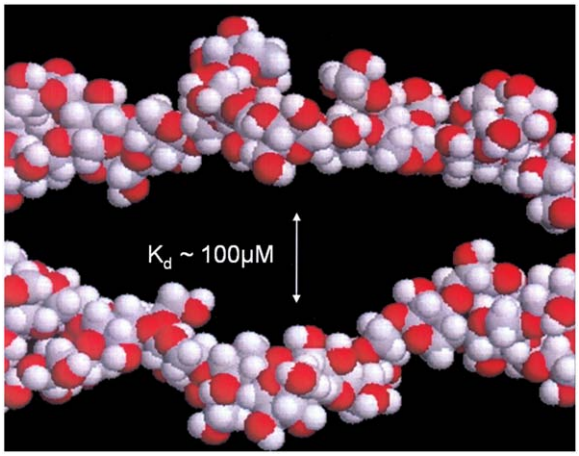

FIGURE 6 Interchain interactions of PO2 and PO5 are of the order 100 μM (adapted from Chapline (82)).

Several works have reported interactions between carbohydrate moieties of glycoprotein/glycolipids, but only in the presence of divalent cations (64–76) and some also have reported effects independent of the presence of salt (61,70,77–80). Bucior and Burger (76) studied the effect of Ca^{2+} concentration and suggested that adhesion force increases (from 310 pN to 375 pN) with increase in Ca^{2+} concentration from 10 mM to 100 mM.

Our finding is, to the best of our knowledge, the first report of a reversible weak self-association both in a polysaccharide and a carbohydrate system not conjugated to a protein. Although this particular weak interaction is not directly important for the bioactive behavior of these substances, the fact that we have demonstrated that carbohydrate groups are capable of weak hydrophilic self-interactions—precisely in the range that others have shown for proteins to be crucial for molecular recognition—makes a significant step forward in our understanding of carbohydrates in both bioactivity and other recognition processes: they may be capable of weak interactions with receptor molecules, whatever they may be.

We thank Professor A. van der Merwe of the Sir William Dunn School of Pathology, Oxford, for helpful discussions and Professor Terje Michaelsen of the Institute of Pharmacy, Oslo, for assistance with the complement activation studies.

This work was supported by the SAS-COST D28 action program of the European Community, the UK Engineering and Physical Sciences Research Council, grant No. GR/S17321/01, and the Slovak Grant Agency (Vedecká Grantová Agentúra), grant No. 2/6131/06.

REFERENCES

1. Watson, J. D. 1970. Molecular Biology of the Gene. W. A. Benjamin, Menlo Park, CA. 102–140.
2. van der Merwe, P. A., and A. N. Barclay. 1994. Transient intercellular adhesion: the importance of weak protein-protein interactions. *Trends Biochem. Sci.* 19:354–358.
3. van der Merwe, P. A., and S. J. Davis. 2003. Molecular interactions mediating T cell antigen recognition. *Annu. Rev. Immunol.* 21:659–684.
4. Vaynberg, J., and J. Qin. 2006. Weak protein-protein interactions as probed by NMR spectroscopy. *Trends Biotechnol.* 24:22–27.
5. Springer, T. A. 1990. Adhesion receptors of the immune system. *Nature.* 346:425–434.
6. Springer, T. A. 1994. Traffic signals for lymphocyte recirculation and leukocyte emigration: the multistep paradigm. *Cell.* 76:301–314.
7. Leishman, A. J., O. V. Naidenko, A. Attinger, F. Koning, C. J. Lena, Y. Xiong, H. C. Chang, E. Reinherz, M. Kronenberg, and H. Cheroutre. 2001. T cell responses modulated through interaction between CD8$\alpha\alpha$ and the nonclassical MHC class I molecule, TL. *Science.* 294:1936–1939.
8. Wyer, J. R., B. E. Willcox, G. F. Gao, U. C. Gerth, S. J. Davis, J. I. Bell, P. A. van der Merwe, and B. K. Jakobsen. 1999. T cell receptor and coreceptor CD8$\alpha\alpha$ bind peptide-MHC independently and with distinct kinetics. *Immunity.* 10:219–225.
9. Kern, P., R. E. Hussey, R. Spoerl, E. L. Reinherz, and H. C. Chang. 1999. Expression, purification, and functional analysis of murine ectodomain fragments of CD8$\alpha\alpha$ and CD8$\alpha\beta$ dimers. *J. Biol. Chem.* 274: 27237–27243.
10. Gao, G. F., B. E. Willcox, J. R. Wyer, J. M. Boulter, C. A. O'Callaghan, K. Maenaka, D. I. Stuart, E. Y. Jones, P. A. Van Der Merwe, J. I. Bell, and B. K. Jakobsen. 2000. Classical and nonclassical class I major histocompatibility complex molecules exhibit subtle conformational differences that affect binding to CD8$\alpha\alpha$. *J. Biol. Chem.* 275:15232–15238.
11. Arcaro, A., C. Gregoire, T. R. Bakker, L. Baldi, M. Jordan, L. Goffin, N. Boucheron, F. Wurm, P. A. van der Merwe, B. Malissen, and I. F. Luescher. 2001. CD8β endows CD8 with efficient coreceptor function by coupling T cell receptor/CD3 to raft-associated CD8/p56(lck) complexes. *J. Exp. Med.* 194:1485–1495.
12. Weber, S., and K. Karjalainen. 1993. Mouse CD4 binds MHC class-II with extremely low affinity. *Int. Immunol.* 5:695–698.
13. Xiong, Y., P. Kern, H. C. Chang, and E. L. Reinherz. 2001. T cell receptor binding to a pMHCII ligand is kinetically distinct from and independent of CD4. *J. Biol. Chem.* 276:5659–5667.
14. Van der Merwe, P. A., A. N. Barclay, D. W. Mason, E. A. Davies, B. P. Morgan, M. Tone, A. K. C. Krishnam, C. Ianelli, and S. J. Davis. 1994. Human cell-adhesion molecule CD2 binds CD58 (LFA-3) with a very-low affinity and an extremely fast dissociation rate but does not bind CD48 or CD59. *Biochemistry.* 33:10149–10160.
15. Silkowski, H., S. J. Davis, A. N. Barclay, A. J. Rowe, S. E. Harding, and O. Byron. 1997. Characterisation of the low affinity interaction between rat cell adhesion molecules CD2 and CD48 by analytical ultracentrifugation. *Eur. Biophys. J.* 25:455–462.
16. Brown, M. H., K. Boles, P. A. van der Merwe, V. Kumar, P. A. Mathew, and A. N. Barclay. 1998. 2B4, the natural killer and T cell immunoglobulin superfamily surface protein, is a ligand for CD48. *J. Exp. Med.* 188:2083–2090.
17. Collins, A. V., D. W. Brodie, R. J. C. Gilbert, A. Iaboni, R. Manso-Sancho, B. Walse, D. I. Stuart, P. A. van der Merwe, and S. J. Davis. 2002. The interaction properties of costimulatory molecules revisited. *Immunity.* 17:201–210.
18. Vales-Gomez, M., H. T. Reyburn, M. Mandelboim, and J. L. Strominger. 1998. Kinetics of interaction of HLA-C ligands with natural killer cell inhibitory receptors. *Immunity.* 9:337–344.
19. Maenaka, K., T. Juji, T. Nakayama, J. R. Wyer, G. F. Gao, T. Maenaka, N. R. Zaccai, A. Kikuchi, T. Yabe, K. Tokunaga, K. Tadokoro, D. I. Stuart, E. Y. Jones, and P. A. van der Merwe. 1999. Killer cell immunoglobulin receptors and T cell receptors bind peptide-major histocompatibility complex class I with distinct thermodynamic and kinetic properties. *J. Biol. Chem.* 274:28329–28334.
20. Wild, M. K., M. C. Huang, U. Schulze-Horsel, P. A. van der Merwe, and D. Vestweber. 2001. Affinity, kinetics, and thermodynamics of E-selectin binding to E-selectin ligand-1. *J. Biol. Chem.* 276:31602–31612.
21. Hakomori, S. 2004. Carbohydrate-to-carbohydrate interaction, through glycosynapse, as a basis of cell recognition and membrane organization. *Glycoconj. J.* 21:125–137.

22. Harding, S. E., and D. J. Winzor. 2001. Sedimentation velocity analytical ultracentrifugation. *In* Protein-Ligand Interactions: Hydrodynamics and Calorimetry. S. E. Harding and B. Z. Chowdhry, editors. Oxford University Press, Oxford, UK. 75–103.

23. Rowe, A. J. 2005. Weak interactions: optimal algorithms for their study in the AUC. *In* Analytical Ultracentrifugation Techniques and Methods. D. J. Scott, S. E. Harding, and A. J. Rowe, editors. Royal Society of Chemistry, Cambridge, UK. 484–500.

24. Kanari, M., M. Tomoda, R. Gonda, N. Shimizu, M. Kimura, M. Kawaguchi, and C. Kawabe. 1989. A reticuloendothelial system-activating arabinoxylan from the bark of *Cinnamomum cassia*. *Chem. Pharm. Bull. (Tokyo).* 37:3191–3194.

25. Samuelsen, A. B., I. Lund, J. M. Djahromi, B. S. Paulsen, J. K. Wold, and S. H. Knutsen. 1999. Structural features and anti-complementary activity of some heteroxylan polysaccharide fractions from the seeds of *Plantago major L. Carbohydr. Polym.* 38:133–143.

26. Ogawa, K., M. Takeuchi, and N. Nakamura. 2005. Immunological effects of partially hydrolyzed arabinoxylan from corn husk in mice. *Biosci. Biotechnol. Biochem.* 69:19–25.

27. Ghoneum, M., and A. Jewett. 2000. Production of tumor necrosis factor-α and interferon-γ from human peripheral blood lymphocytes by MGN-3, a modified arabinoxylan from rice bran, and its synergy with interleukin-2 in vitro. *Cancer Detect. Prev.* 24:314–324.

28. Ebringerová, A., and T. Heinze. 2000. Xylan and xylan derivatives—biopolymers with valuable properties, 1. Naturally occurring xylans structures, isolation procedures and properties. *Macromol. Rapid Commun.* 21:542–556.

29. Ebringerova, A., Z. Hromadkova, and V. Hribalova. 1995. Structure and mitogenic activities of corn cob heteroxylans. *Int. J. Biol. Macromol.* 17:327–331.

30. Zhang, P. Y., J. L. Wampler, A. K. Bhunia, K. M. Burkholder, J. A. Patterson, and R. L. Whistler. 2004. Effects of arabinoxylans on activation of murine macrophages and growth performance of broiler chicks. *Cereal Chem.* 81:511–514.

31. Fincher, G. B., and B. A. Stone. 1986. Cell walls and their components in cereal grain technology. *In* Advances in Cereal Science and Technology. Y. Pomeranz, editor. American Association of Cereal Chemists, St. Paul, MN. 207–295.

32. Rao, M. V. S. S. T., and G. Muralikrishna. 2001. Non-starch polysaccharides and bound phenolic acids from native and malted finger millet (Ragi, Eleusine coracana, Indaf-15). *Food Chem.* 72:187–192.

33. Ishii, T. 1997. Structure and functions of feruloylated polysaccharides. *Plant Sci.* 127:111–127.

34. Ahluwalia, B., and S. C. Fry. 1986. Barley endosperm cell-walls contain a feruloylated arabinoxylan and a non-feruloylated beta-glucan. *J. Cereal Sci.* 4:287–295.

35. Smith, M. M., and R. D. Hartley. 1983. Occurrence and nature of ferulic acid substitution of cell-wall polysaccharides in graminaceous plants. *Carbohydr. Res.* 118:65–80.

36. Ebringerova, A., and Z. Hromadkova. 2002. Effect of ultrasound on the extractability of corn bran hemicelluloses. *Ultrason. Sonochem.* 9: 225–229.

37. Schooneveld-Bergmans, M. E. F., A. M. C. P. Hopman, G. Beldman, and A. G. J. Voragen. 1998. Extraction and partial characterization of feruloylated glucuronoarabinoxylans from wheat bran. *Carbohydr. Polym.* 35:39–47.

38. Kanari, M., M. Tomoda, R. Gonda, N. Shimizu, M. Kimura, M. Kawaguchi, and C. Kawabe. 1989. A reticuloendothelial system-activating arabinoxylan from the bark of Cinnamomum cassia. *Chem. Pharm. Bull. (Tokyo).* 37:3191–3194.

39. Ogawa, K., M. Takeuchi, and N. Nakamura. 2005. Immunological effects of partially hydrolyzed arabinoxylan from corn husk in mice. *Biosci. Biotechnol. Biochem.* 69:19–25.

40. Ghoneum, M., and A. Jewett. 2000. Production of tumor necrosis factor-α and interferon-γ from human peripheral blood lymphocytes by MGN-3, a modified arabinoxylan from rice bran, and its synergy with interleukin-2 in vitro. *Cancer Detect. Prev.* 24:314–324.

41. Schachman, H. K. 1989. Analytical ultracentrifugation reborn. *Nature.* 341:259–260.

42. Rowe, A. J. 1977. Concentration dependence of transport. *Biopolymers.* 16:2595–2611.

43. Gill, P. E., and W. Murray. 1978. Algorithms for the solution of the nonlinear least-squares problem. *Siam J. Numer. Anal.* 15:977–992.

44. Hromádková, Z., A. Malovíková, A. Ebringerová, N. Vrchotová, T. Patel, and S. E. Harding. 2005. Wheat bran heteroxylan-phenolic complexes and associated antioxidant activity. *3rd European Carbohydrate Symposium, August 21–26, Bratislava, Slovaki.* P089.

45. Green, A. A. 1933. The preparation of acetate and phosphate buffer solutions of known pH and ionic strength. *J. Am. Chem. Soc.* 55:2331–2336.

46. Gomez, C., A. Navarro, P. Manzanares, A. Horta, and J. V. Carbonell. 1997. Physical and structural properties of barley $(1\rightarrow3),(1\rightarrow4)$-[$\beta$]–glucan. Part I. Determination of molecular weight and macromolecular radius by light scattering. *Carbohydr. Polym.* 32:7–15.

47. Hromadkova, Z., and A. Ebringerova. 2003. Ultrasonic extraction of plant materials—investigation of hemicellulose release from buckwheat hulls. *Ultrason. Sonochem.* 10:127–133.

48. Izydorczyk, M. S., and C. G. Biliaderis. 1994. Studies on the structure of wheat-endosperm arabinoxylans. *Carbohydr. Polym.* 24:61–71.

49. Iribe, H., and T. Koga. 1984. Augmentation of the proliferative response of thymocytes to phytohemagglutinin by the muramyl dipeptide. *Cell. Immunol.* 88:9–15.

50. Ebringerova, A., A. Kardosova, Z. Hromadkova, and V. Hribalova. 2003. Mitogenic and comitogenic activities of polysaccharides from some European herbaceous plants. *Fitoterapia.* 74:52–61.

51. Michaelsen, T. E., A. Gilje, A. B. Samuelsen, K. Hogasen, and B. S. Paulsen. 2000. Interaction between human complement and a pectin type polysaccharide fraction, PMII, from the leaves of *Plantago major L. Scand. J. Immunol.* 52:483–490.

52. Nergard, C. S., H. Kiyohara, J. C. Reynolds, J. E. Thomas-Oates, T. Matsumoto, H. Yamada, T. Patel, D. Petersen, T. E. Michaelsen, D. Diallo, and B. S. Paulsen. 2006. Structures and structure-activity relationships of three mitogenic and complement fixing pectic arabinogalactans from the malian antiulcer plants *Cochlospermum tinctorium A. Rich* and *Vernonia kotschyana Sch. Bip.* ex Walp. *Biomacromolecules.* 7:71–79.

53. Schuck, P. 1998. Sedimentation analysis of noninteracting and self-associating solutes using numerical solutions to the Lamm equation. *Biophys. J.* 75:1503–1512.

54. Schuck, P., and P. Rossmanith. 2000. Determination of the sedimentation coefficient distribution by least-squares boundary modeling. *Biopolymers.* 54:328–341.

55. Laue, T. M., B. D. Shah, T. M. Ridgeway, and S. L. Pelletier. 1992. Computer-aided interpretation of analytical sedimentation data for proteins. *In* Analytical Ultracentrifugation in Biochemistry and Polymer Science. S. E. Harding, A. J. Rowe, and J. C. Horton, editors. Royal Society of Chemistry, Cambridge, UK. 90–125.

56. Gilbert, L. M., and G. A. Gilbert. 1973. Sedimentation velocity measurement of protein association. *In* Methods in Enzymology. C. H. W. Hirs and S. N. Timasheff, editors. Academic Press, New York. 273–296.

57 Rowe, A. J. 1979. Euromech 120 (Abstracts), 5.3.

58. Rowe, A. J. 1992. The concentration dependence of sedimentation. *In* Analytical Ultracentrifugation in Biochemistry and Polymer Science. S. E. Harding, A. J. Rowe, and J. C. Horton, editors. Royal Society of Chemistry, Cambridge, UK. 394–406.

59. Jacobs, D., and D. Morrison. 1977. Inhibition of the mitogenic response to lipopolysaccharide (LPS) in mouse spleen cells by polymyxin B. *J. Immunol.* 118:21–27.

60. Tanford, C. 1980. The Hydrophobic Effect: Formation of Micelles and Biological Membranes. Wiley Interscience, New York.

61. Santacroce, P. V., and A. Basu. 2004. Studies of the carbohydrate-carbohydrate interaction between lactose and GM_3 using Langmuir monolayers and glycolipid micelles. *Glycoconj. J.* 21:89–95.

62. Basu, A. 2006. http://www.brown.edu/Research/Basu_Research_Group. 02/02/2006.

63. Harding, S. E. 2005. Challenges for the modern analytical ultracentrifuge analysis of polysaccharides. *Carbohydr. Res.* 340:811–826.

64 Stewart, R. J., and J. M. Boggs. 1993. A carbohydrate-carbohydrate interaction between galactosylceramide-containing liposomes and cerebroside sulfate-containing liposomes: dependence on the glycolipid ceramide composition. *Biochemistry.* 32:10666–10674.

65. Kojima, N., and S. Hakomori. 1989. Specific interaction between gangliotriaosylceramide (Gg3) and sialosyllactosylceramide (GM3) as a basis for specific cellular recognition between lymphoma and melanoma cells. *J. Biol. Chem.* 264:20159–20162.

66. Armin, G., C. Gege, and R. R. Schmidt. 2000. Calcium-dependent carbohydrate-carbohydrate recognition between lewis^x blood group antigens. *Angew. Chem. Int. Ed. Engl.* 39:3245–3249.

67. Kojima, N., B. Fenderson, M. Stroud, R. Goldberg, R. Habermann, T. Toyokuni, and S.-I. Hakomori. 1994. Further studies on cell adhesion based on Le^x-Le^x interaction, with new approaches: embryoglycan aggregation of F9 teratocarcinoma cells, and adhesion of various tumour cells based on Le^x expression. *Glycoconj. J.* 11:238–248.

68. Fenderson, B., U. Zehavi, and S. Hakomori. 1984. A multivalent lacto-N-fucopentaose III-lysyllysine conjugate decompacts preimplantation mouse embryos, while the free oligosaccharide is ineffective. *J. Exp. Med.* 160:1591–1596.

69. Eggens, I., B. Fenderson, T. Toyokuni, B. Dean, M. Stroud, and S. Hakomori. 1989. Specific interaction between Le^x and Le^x determinants. A possible basis for cell recognition in preimplantation embryos and in embryonal carcinoma cells. *J. Biol. Chem.* 264:9476–9484.

70. Cavallaro, U., and G. Christofori. 2004. Cell adhesion and signalling by cadherins and Ig-CAMs in cancer. *Nat. Rev. Cancer.* 4:118–132.

71. Kojima, N., and S. Hakomori. 1991. Cell adhesion, spreading, and motility of GM3-expressing cells based on glycolipid-glycolipid interaction. *J. Biol. Chem.* 266:17552–17558.

72. Menikh, A., P. G. Nyholm, and J. M. Boggs. 1997. Characterization of the interaction of Ca^{2+} with hydroxy and non-hydroxy fatty acid species of cerebroside sulfate by Fourier transform infrared spectroscopy and molecular modeling. *Biochemistry.* 36:3438–3447.

73. Humphreys, T. 1963. Chemical dissolution and in vitro reconstruction of sponge cell adhesions: I. Isolation and functional demonstration of the components involved. *Dev. Biol.* 8:27–47.

74. Henkart, P., S. Humphreys, and T. Humphreys. 1973. Characterization of sponge aggregation factor. A unique proteoglycan complex. *Biochemistry.* 31:3045–3050.

75. Jumblatt, J. E., V. Schlup, and M. M. Burger. 1980. Cell-cell recognition: specific binding of Microciona sponge aggregation factor to homotypic cells and the role of calcium ions. *Biochemistry.* 19: 1038–1042.

76. Bucior, I., and M. M. Burger. 2004. Carbohydrate-carbohydrate interaction as a major force initiating cell-cell recognition. *Glycoconj. J.* 21:111–123.

77 Matsuura, K., R. Oda, H. Kitakouji, M. Kiso, K. Kitajima, and K. Kobayashi. 2004. Surface plasmon resonance study of carbohydrate-carbohydrate interaction between various gangliosides and Gg3-carrying polystyrene. *Biomacromolecules.* 5:937–941.

78. Turner, S. R., and M. M. Burger. 1973. Involvement of a carbohydrate group in the active site for surface guided reassociation of animal cells. *Nature.* 244:509–510.

79. Yu, S., N. Kojima, S.-I. Hakomori, S. Kudo, S. Inoue, and Y. Inoue. 2002. Binding of rainbow trout sperm to egg is mediated by strong carbohydrate-to-carbohydrate interaction between (KDN)GM3 (deaminated neuraminyl ganglioside) and Gg3-like epitope. *Proc. Natl. Acad. Sci. USA.* 99:2854–2859.

80. Song, Y., D. A. Withers, and S. Hakomori. 1998. Globoside-dependent adhesion of human embryonal carcinoma cells, based on carbohydrate-carbohydrate interaction, initiates signal transduction and induces enhanced activity of transcription factors AP1 and CREB. *J. Biochem. (Tokyo).* 273:2517–2525.

81. Adom, K. K., and R. H. Liu. 2002. Antioxidant activity of grains. *J. Agric. Food Chem.* 50:6182–6187.

82. Chaplin, M. 2006. http://www.lsbu.ac.uk/water/hyara.html. 06/06/2006.